Max-Planck-Institut
für Mathematik
in den Naturwissenschaften
Leipzig

Actin Dynamics and Cell Motility: Minimal Models for the Initiation of Cell Movement

by

Jan Fuhrmann, Josef Käs, and Angela Stevens

Preprint no.: 99 2006

ACTIN DYNAMICS AND CELL MOTILITY: MINIMAL MODELS FOR THE INITIATION OF CELL MOVEMENT

JAN FUHRMANN[1] AND JOSEF KÄS[2] AND ANGELA STEVENS[1]

ABSTRACT. The actin driven motility of eukaryotic cells has been one of the most rapidly developing research areas in biology over the last decades. Polymerization and depolymerization of filaments is the driving force behind the crawling motion of individual cells. There is a large variety of proteins known or suspected to be involved in this polymerization machinery. The question arises which of them are essential for the ability of a cell to move directionally. Many studies have been conducted on cells which are already in motion - or at least polarized with established lamellipods, and several mechanisms have been shown to be essential for sustaining the large movement velocities observed in vivo. The question we addressed here is what minimal requirements have to be met by a non polarized resting cell to react to an external stimulus in a prescribed direction.

For that purpose, we develop a minimal model for actin turnover, examine its steady states, and try to figure out which types of perturbations are most appropriate to turn the cytoskeleton into a polarized state which may be viewed as the beginning of directed motion. We analyze a one dimensional model for a resting cell describing the actin network therein. For the time being we restrict ourselves to describing the dynamics of barbed ends accumulating near the cell membrane. Pushing the membrane forward and establishing a lamellipod would be the next step in the initiation of movement and shall be investigated in future.

In our simulations we found that very few mechanisms are sufficient to create a significant modification of the cytoskeleton. Moreover we see a striking effect of the diffusion coefficient for the actin monomers on the strength of this modification.

1. INTRODUCTION

The role of actin dynamics in the directed motion of eucaryotic cells is a topic of intensive experimental investigations for nearly half a century (compare [7]). Especially in light of recent investigations on cell movement and mechanosensing in early development, tumor growth and certain disease states, it is of utmost importance to understand the main underlying principles of cytoskeleton dynamics involved in these processes. One main aim is to predict and control actin dynamics in a variety of experimental contexts. Parallel to the experiments also theoretical modeling of filament driven cell locomotion started in the 1960's, e.g. in [2] and [19]. Current mathematical models often consider cells which are already moving, or at least have established extensions of filopods or lamellipodia as described in [9], [15], or [18], or concentrate on resting but already polarized cells with protrusions, e.g. in [3]. Here we want to find a minimal model for the transition of a non polarized resting state of a cell into a motile state which is characterized by the switch from a symmetric to an asymmetric distribution of the actin cytoskeleton.

During cell movement a constant turnover of actin monomers takes place. They polymerize and depolymerize at the filament ends, with an average preference of polymerizing at barbed ends and depolymerizing at pointed ones. This process called treadmilling is explained in detail in section 1.1. It is observed though that even resting cells perform treadmilling and thus use a large amount of energy without an obvious reason. So major questions in this context are, why this is the case, and what kind of perturbations of the treadmilling process are needed to allow for a resting cell to move.

[1]Max-Planck-Institute for Mathematics in the Sciences
[2]Physics Department, Leipzig University

In [5] Carlier et al. discuss several mechanisms to be necessary for the fast actin driven cell locomotion observed in vivo. These are barbed end capping, monomer sequestering, and filament severing by ADF/cofilin. We will address these mechanisms as perturbations of the equilibrium distribution of actin filaments in a resting cell later on.

In this paper we describe a resting model-cell which should prepare to crawl into the direction of an external stimulus. We aim to determine minimal requirements for the initiation of this movement. That is, we want to find mechanisms enabling the cell to break the symmetry of the steady state distribution of actin filaments by applying as simple perturbations as possible. We do not address the question if a similar effect could be observed in models without treadmilling during the resting stage of the cell, or if the effect would vary in strength in this case. An answer to this would provide an insight into the question why treadmilling may be useful and will be explored in the future. Here we first want to understand the effects of different known dynamics.

Specific experiments we can address with our model are those e.g. by Döbereiner and Sheetz [8] concerning cell spreading. Our resting model cell would then correspond to a fibroblast sinking down in a basin filled with nutrient solution. Its landing on the fibronectin coated ground would be the stimulus. This is in fact a symmetric perturbation if the substrate is homogeneously coated and completely flat. In this case the cell will spread on the surface in a rotationally symmetric manner. If the coating with fibronectin is considered to be only partial one could imagine a cell landing on the edge of a coated area and a directed stimulus would be established (see [6]).

In this section we will set up a one dimensional continuum model for actin monomers and filament ends. The G-actin density will be described by a reaction diffusion equation and the end densities by conservation laws. In section 2 we briefly discuss the existence and shape of steady states of the system which correspond to a resting cell. Section 3 is devoted to the numerical treatment of the model, particularly with regard to perturbations of the resting state. The simulations show some remarkable results which are discussed in section 4. Perturbations of the reaction parameters and local monomer release are capable of redistributing the barbed filament ends towards the cell membrane - an effect which is considerably affected by the value of the diffusion coefficient for the actin monomers. This result gives rise to questions concerning the diffusive nature of monomer dynamics. In the end we give a short outlook on possible extensions of our model as well as open questions to be addressed by experiments or further theoretical investigation.

1.1. **The Model Ingredients.** Having in mind the descriptions in [9] and [15] we discuss a one dimensional model for the dynamics of actin monomers and filaments. The latter have two types of ends exhibiting different reaction kinetics. Actin monomers show a high affinity to barbed ends where they are preferentially polymerized. This results in an average elongation of the filament. At the pointed ends depolymerization dominates and the filaments shorten there in average. We therefore assign an orientation to each actin filament, namely "right oriented" for those having their barbed ends pointing to the right and "left oriented" for those growing to the left. The monomer turnover then leads to a seemingly directed movement of filaments, which is balanced by a myosin driven pullback, denoted as retrograde flow. In equilibrium - corresponding to a resting cell - this flow should exactly compensate the movement resulting from treadmilling. We will later mention some additional proteins involved in the regulation of actin dynamics.

1.2. **Model Variables and Parameters.** We consider a resting cell on a homogeneous substrate where the direction of motion shall be the (positive) x-axis. An initially non polarized cell is rotationally symmetric. After having chosen this direction of polarization, the shape of the cell

is symmetric with respect to the y-coordinate, which justifies a one dimensional model as a first ansatz. The cell is thus occupying an interval on the real line, say $Cell = \left(-\frac{L}{2}, \frac{L}{2}\right)$. Since we do not consider forces acting at the cell membrane in this paper, we leave this interval fixed during our simulations. We want to analyze the differences in accumulation of barbed ends at the membrane under a variety of conditions, in order to judge the respective strength of effect. Our aim is to understand which perturbations of the actin dynamics are suitable to drive the cell into motion.

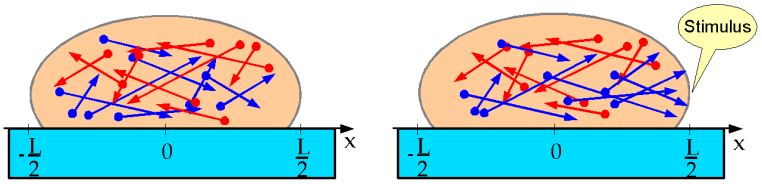

FIG. 1. *left*: Non polarized cell on a flat substrate, barbed (denoted by arrows) and pointed (points) ends are distributed symmetrically for the respective filament orientations (red: left oriented filaments, blue: right oriented filaments); *right*: Upon a stimulus for movement to the right the barbed ends of the right oriented filaments accumulate at the cell membrane, ready to push it forward and thus create a lamellipod.

In the following we denote the concentration of actin monomers by a and those of the filament ends by B_r, B_l for the barbed ends pointing to the right and left, respectively, and P_r, P_l for the pointed ends. The length of the different filaments is not explicitly modeled but the average length distribution can be calculated from this, as we shall see later.

Unit Conversion. Naturally concentrations are given in $\mu M = \mu mol/l$. We transform this into the one dimensional unit μm^{-1} (read: $parts\,per\,\mu m$). Assuming for simplicity a square shaped cell with a length and width of $L = 20\,\mu m$, and a height of $10\,\mu m$ this leads to a conversion factor

$$\eta = 1.2 \cdot 10^5\,\mu m^{-1}\mu M^{-1}, \tag{1.1}$$

i.e., $1\,\mu M \hat{=} 1.2 \cdot 10^5\,\mu M^{-1}$. Different spatial extensions in one or the other direction would change this factor linearly, so that the assumption of a constant cell cross section is reasonable as long as we do not consider lamellipodia or filopodia which alter the cell shape significantly. Moreover, the concrete value of η only affects the values of the results but not the shape since the conversion factor is canceled in each term of the equations.

The reaction kinetics at the filament ends are characterized by the reaction rates κ^B and κ^P and by critical concentrations a_B and a_P for the barbed and pointed ends, respectively. First these are considered to be constant and will later be varied spatially, depending on the type of perturbation due to the external signal. The elongation of a filament due to polymerization of a single monomer is denoted by $\delta = 2.2\,nm$, the retrograde flow velocity by v_R. Finally the monomers are assumed to undergo diffusion with a diffusion coefficient D.

1.3. **The Model.** Consider a barbed end of a right oriented filament which at time t is located at position x. Within a timestep Δt it will be pulled back to the left by $-v_R\Delta t$, due to the retrograde flow. If a monomer is attached or detached within that timestep the position additionally changes by $\pm\delta$. Taking the reaction kinetics into account the mean velocity is then given by

$$v_B = -v_R + \delta\kappa^B(a - a_B). \tag{1.2}$$

Thus the concentration of right oriented barbed ends is governed by a conservation law

$$\partial_t B_r = \partial_x\left[\left(v_R - \delta\kappa^B(a - a_B)\right)B_r\right] \equiv -\partial_x\left(v_B(a)B_r\right). \tag{1.3}$$

Similarly the equations for the other types of ends can be derived:

$$\partial_t B_l = -\partial_x \left[\left(v_R - \delta \kappa^B (a - a_B) \right) B_l \right] \equiv \partial_x \left(v_B(a) B_l \right)$$
$$\partial_t P_r = \partial_x \left[\left(v_R + \delta \kappa^P (a - a_P) \right) P_r \right] \equiv -\partial_x \left(v_P(a) P_r \right)$$
$$\partial_t P_l = -\partial_x \left[\left(v_R + \delta \kappa^P (a - a_P) \right) P_l \right] \equiv \partial_x \left(v_P(a) P_l \right).$$

If we assume that branching, nucleation, or severing of filaments do not happen, the total number of ends of each type is conserved within the cell. This is clearly true also in our model system provided with homogeneous DIRICHLET boundary values

$$B_{r/l} \mid_{x=\pm\frac{L}{2}} = 0. \tag{1.4}$$

These boundary conditions are motivated by the fact that the interaction of barbed ends with the membrane is not modeled here. Therefore these ends should not be directly located at the cell membrane which will be achieved by choosing initial conditions with compact support. The minimal time of unique existence of a solution can then be estimated from the distance of this support to the boundary and an upper bound for the velocities v_B, v_P.

The monomer density is described by a reaction diffusion equation including the reaction kinetics at the barbed and pointed ends:

$$\partial_t a = D\, \partial_{xx} a - \kappa^B (a - a_B)(B_r + B_l) - \kappa^P (a - a_P)(P_r + P_l). \tag{1.5}$$

The monomers are assumed to be reflected at the cell membrane. We therefore prescribe no-flux boundary conditions

$$\partial_x a \mid_{x=\pm\frac{L}{2}} = 0. \tag{1.6}$$

The density and the average length of the filaments of either orientation can be computed from the concentrations of the ends. Since our model does not include mechanisms of creation or destruction of filaments, their total number $N_i = \int_{Cell} B_i \mathsf{d}x = \int_{Cell} P_i \mathsf{d}x \, (i = l, r)$ is conserved and the average filament length $\bar{l}_i$ is directly related to the F-actin amount F_i (see 1.8), namely

$$\bar{l}_i = \frac{F_i}{N_i} \delta.$$

In the symmetric case of an initially non polarized cell there are as many right oriented filaments as left oriented ones and the additional simplification $N_r = N_l = N$ holds.

The number of filaments at the position x is given by

$$f(x) = f_r(x) + f_l(x) = \int_x^{\frac{L}{2}} B_r - P_r \mathsf{d}x' + \int_x^{\frac{L}{2}} P_l - B_l \mathsf{d}x'. \tag{1.7}$$

Each filament contains $\frac{l_0}{\delta}$ monomers per unit length l_0. The total amount of actin monomers assembled in filaments therefore is

$$F = F_r + F_l = \int_{Cell} f_r \frac{\mathsf{d}x}{\delta} + \int_{Cell} f_l \frac{\mathsf{d}x}{\delta} = \int_{Cell} f \frac{\mathsf{d}x}{\delta} = \int_{Cell} \int_x^{\frac{L}{2}} \frac{B_r - P_r + P_l - B_l}{\delta} \mathsf{d}x' \mathsf{d}x. \tag{1.8}$$

So the end densities can be rescaled by a factor of $\frac{1}{\delta}$, so that they are given in μm^{-2}. As a result an additional factor δ has to be incorporated into the equation for the monomers:

$$\partial_t a = D\, \partial_{xx} a - \delta\, \kappa^B (a - a_B)(B_r + B_l) - \delta\, \kappa^P (a - a_P)(P_r + P_l). \tag{1.9}$$

Summarizing the variables and parameters used in our model we obtain

variables	description	value	unit
x	spatial variable	$x \in \left[-\frac{L}{2}, \frac{L}{2}\right]$	μm
t	time	$t \geq 0$	s
$a(t, x)$	monomer density	$a \geq 0$	μm^{-1}
$B_{r/l}(t, x)$	concentration of right/left oriented barbed ends	$B_{r/l} \geq 0$	μm^{-2}
$P_{r/l}(t, x)$	concentration of right/left oriented pointed ends	$P_{r/l} \geq 0$	μm^{-2}
parameters			
a_B	critical monomer concentration at barbed ends	$9.6 \cdot 10^3$	μm^{-1}
a_P	critical monomer concentration at pointed ends	$6 \cdot 10^4$	μm^{-1}
κ^B	reaction rate at barbed ends	$\frac{1}{\delta}\frac{5}{12}10^{-4}$	$\mu m\, s^{-1}$
κ^P	reaction rate at pointed ends	$\frac{1}{\delta}\frac{5}{24}10^{-5}$	$\mu m\, s^{-1}$
δ	filament elongation by addition of one monomer	0.0022	μm
D	diffusion coefficient for monomers	30	$\mu m^2 s^{-1}$
L	cell size	20	μm
v_R	retrograde flow velocity	0.1	$\mu m\, s^{-1}$

TABLE 1: Model variables and parameters.

2. Conservation of Mass and Steady States

2.1. **Conservation of Mass.** The total actin mass, that is the sum of F- and G-actin masses, in our model is conserved. It is computed by

$$A = G + F = \int_{Cell} a + \frac{f}{\delta} \mathrm{d}x = \int_{Cell} \left[a + \int_x^{\frac{L}{2}} B_r - P_r + P_l - B_l \mathrm{d}x' \right] \mathrm{d}x. \tag{2.1}$$

One can easily show that $\partial_t A = 0$ by expressing the time derivatives of the densities in (2.1) by the right hand sides of the model equations and employing the respective boundary conditions stated in the previous section.

2.2. **Steady States.** Since we want to investigate a resting cell which prepares to move upon a stimulus, we first calculate the steady states of our model equations, namely

$$0 = \partial_x (v_B B_r) \tag{2.2}$$

and analogously for the equations for the other filament ends. For the monomers consider

$$0 = D\, \partial_{xx} a - \delta\, \kappa^B (a - a_B)(B_r + B_l) - \delta\, \kappa^P (a - a_P)(P_r + P_l). \tag{2.3}$$

Due to the homogeneous DIRICHLET boundary conditions on the ends no homogeneous steady states do exist, except for the trivial case where all end densities vanish and there are no filaments at all inside the cell.

However, the equations for the ends can be solved by arbitrary functions with zero boundary conditions if the velocities

$$v_B = v_R - \delta \kappa^B (a - a_B) \tag{2.4}$$

and

$$v_P = v_R + \delta \kappa^P (a - a_P), \tag{2.5}$$

respectively, vanish identically. This leads to the following condition for the steady state concentration of monomers a^{ss}

$$\kappa^B (a^{ss} - a_B) = \frac{v_R}{\delta} = \kappa^P (a_P - a^{ss}), \tag{2.6}$$

which, in fact, are two conditions. Together they give a consistency postulation for the reaction rates and the critical concentrations in equilibrium. Thus

$$a^{ss} = \frac{\kappa^B a_B + \kappa^P a_P}{\kappa^B + \kappa^P} \tag{2.7}$$

is the weighted mean of the critical concentrations.

The monomer equation leads to a pointwise algebraic condition for the end densities:

$$B_r + B_l = P_r + P_l. \tag{2.8}$$

Additionally, the resting cell shall not be polarized and therefore we have the symmetry conditions

$$B_r(x,\,t) = B_l(-x,\,t) \qquad \text{and} \qquad P_r(x,\,t) = P_l(-x,\,t) \qquad \textit{for all } (x,\,t). \tag{2.9}$$

All conditions can be satisfied at least by the following two settings. Given an arbitrary distribution for B_r with homogeneous boundary conditions, we set $B_l(x,\,t) = B_r(-x,\,t)$ and

1. $P_r = B_l$, $P_l = B_r$, or
2. $P_r = P_l = \frac{1}{2}(B_r + B_l)$.

3. Perturbations of the Steady States and Computational Treatment

3.1. **General Setting.** For our simulations the interval representing the cell is divided into N segments of length $\Delta x = \frac{L}{N}$, the time is measured in K steps of length Δt. In what follows, x_i denotes the i-th lattice point, that is $x_i = -\frac{L}{2} + i\Delta x$, $i = 0, \ldots, N$.

First we implement the steady states as bell shaped C_c^∞-functions (w.r.t. x) of the type

$$B^k_{r,i} \equiv B_r(x_i,\,t_k) = c\,\exp\left[\frac{\alpha w^2}{\left(\frac{i}{N} - \frac{i_0}{N}\right)^2 - w^2}\right] \quad \textit{for } i = i_0 - w\,N, \ldots,\, i_0 + w\,N,\, k \in \mathbb{N} \tag{3.1}$$

with a peak of width $2w$ around x_{i_0}. The positive constants c, α are chosen such that in the steady state the total amounts of filamentous and globular actin are about the same, which is often assumed for resting cells, e.g. fibroblasts (see [1]).

For the numerical simulation we assume that the monomer dynamics is much faster than that of the filament ends. This allows us to decouple the equations. For each timestep we thus first compute the new monomer distribution and then use this for the calculation of the new end densities.

The monomer concentration is discretized by forward differences in time and central differences in space to generate an implicit finite difference scheme. The coefficient matrix of the resulting system of linear equations is a symmetric tridiagonal matrix which can be inverted by an algorithm of complexity $\mathcal{O}(N)$ without Pivot search.

For the conservation laws describing the end densities we used a varied Lax-Wendroff-scheme. If the density itself is for the moment denoted by u and the velocity term by v our equations are of type $\partial_t u = \partial_x(vu)$. Together with the Taylor expansion of u w.r.t. time this leads to

$$\partial_{tt} u = \partial_{tx}(vu) = v\partial_{xx}u + \partial_x v \partial_x(vu) + \partial_x u \partial_t v + u\partial_{tx} v, \tag{3.2}$$

where the spatial derivatives of u and v are implemented by central differences and the temporal derivatives of the velocity is discretized by forward differences. The velocity depends on the new monomer density, which has already been computed.

After each timestep we compute the filament length distributions and the masses of filamentous and globular actin.

3.2. **Perturbations of Steady States.** To enable the cell to move, perturbations of the steady states are applied. This can be modeled by a number of mechanisms. In the setting of cell spreading we can address two basic types of stimuli, namely symmetric and asymmetric ones. The first one appears if the surface the cell lands on is considered to be homogeneous. Then the center of the cell hits this surface and attaches to it under pressure whereas at its edges the membrane is pulled down towards the ground by adhesions as can be seen in figure 2 on the left. The case of asymmetric perturbations may occur if the cell lands on an inhomogeneous substrate with spatially varying adhesion properties. For instance, it is a big difference for fibroblasts whether the surface they are sitting on is glossy or coated with fibronectin (see fig. 2, right). Here we assume that the stimulus acting on the cell is directed to the right, i.e., the cell shall be animated to move in positive x-direction.

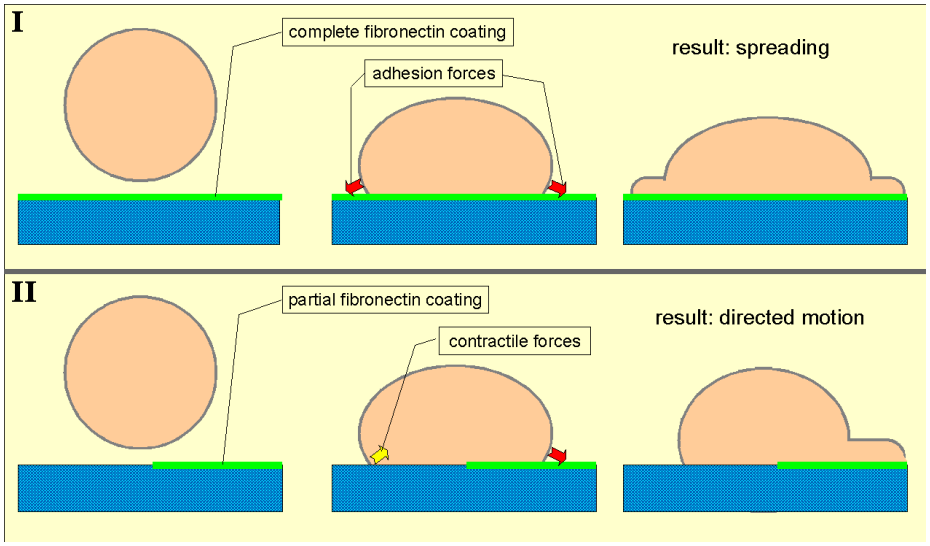

FIG. 2: CELL SPREADING. *I)* Cells landing on a surface completely coated with fibronectin tend to spread symmetrically; *II)* Landing on the border of a coated domain causes the cell to move towards the fibronectin covered part.

The "success" of the perturbation will be measured by the extent of accumulation of right oriented barbed ends near the right cell boundary in case of a directed stimulus (corresponding to case *II)* in fig. 2). These would then in principle be able to push the membrane forward in the desired direction of crawling. In case of a symmetric perturbation we would expect the right and left oriented barbed ends to accumulate near the right or left cell membrane, respectively. In the sequel we explain specific perturbations.

Perturbation of the monomer density. The easiest way to perturb the system is a variation of the monomer distribution. There are two options for this, namely the local release of additional monomers or the redistribution of the available ones. The former effect may result from the release of monomers from vesicles which dissolve upon the external stimulus. The latter effect could be accomplished by a directed transport of G-actin, where vesicles may be used as well. Mathematically we model the first case by adding a bell shaped peak of actin monomers - as already described in (3.1) - to the homogeneous steady state concentration. We locate the peak near the membrane on that side of the domain the cell is supposed to move to.

The second case is modeled similarly, but now the constant offset is lower than the steady state concentration since the monomers assembled in the peak have been gathered from the

monomers available within the cell. The total amount of G-actin remains unaltered in this setting.

Perturbation of reaction rates and critical concentrations. Instead of constant reaction rates and constant critical concentrations we may assume that they vary in space and time. The cell could accomplish this by local variations of salt concentrations, the pH-value, the availability of ATP, or by the use of sequestering agents or other actin related proteins. Also ADF/cofilin can be viewed in this context as causing higher reactivity and therefore stronger depolymerization at the pointed ends. We concretely implement this variation by an arctan-distribution of reaction rates and critical concentrations of the form

$$k_i \equiv k(x_i) = k^0 \left(\frac{\pi}{2} \pm \arctan\left[\mu \frac{i - i_0}{N} \right] \right). \tag{3.3}$$

For the description of cell spreading the perturbations have to be applied symmetrically which can be done by superimposing two such ARCTAN curves.

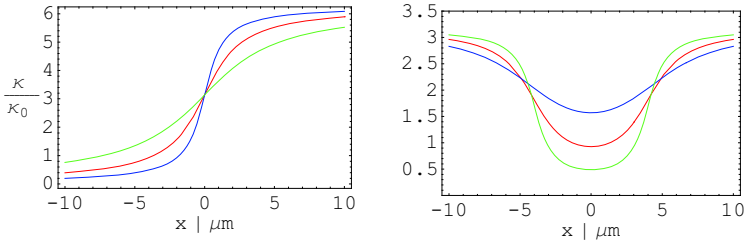

FIG. 3. PERTURBATIONS OF THE REACTION RATES. left: asymmetric case, right: symmetric case. Steeper curves correspond to larger values of μ in 3.3, i_0 is chosen to be $N/2$, i.e., in the center of the cell. The perturbations of the critical concentrations look similar.

Capping. The capping of barbed ends by several capping proteins prevents them from taking part in the reaction kinetics and is often considered essential for cell motility (see [5]). As a first ansatz we introduce an artificial capping rate γ, the (spatially variable) percentage of barbed ends which are capped. These capped barbed ends simply underly transport by the retrograde flow, whereas the free barbed ends act as before. A more complex but also more adequate method of treating the capping problem would be to introduce a capping protein concentration as an additional variable into the model. The cappers would then be governed by a reaction diffusion equation similar to that for the monomers and lead to additional reaction terms in the barbed end equations which would now have to be divided into capped and free (active) ones. The respective model equations read

$$\partial_t B_r^a = \partial_x \left[\left(v_R - \delta\, \kappa^B (a - a_B) \right) B_r^a \right] - \gamma_+ c\, B_r^a + \gamma_- B_r^c$$

$$\partial_t B_l^a = -\partial_x \left[\left(v_R - \delta\, \kappa^B (a - a_B) \right) B_l^a \right] - \gamma_+ c\, B_l^a + \gamma_- B_l^c$$

for the active barbed ends and

$$\partial_t B_r^c = v_R \partial_x B_r^c + \gamma_+ c\, B_r^a - \gamma_- B_r^c$$

$$\partial_t B_l^c = -v_R \partial_x B_l^c + \gamma_+ c\, B_l^a - \gamma_- B_l^c$$

for the capped barbed ends where $\gamma_\pm$ are the reaction rates for capping and uncapping and c denotes the density of the capping protein governed by the reaction diffusion equation

$$\partial_t c = \tilde{D} \partial_{xx} c - \gamma_+ c \left(B_r^a + B_l^a \right) + \gamma_- \left(B_r^c + B_l^c \right).$$

In the equation describing the monomer density we only have to replace the barbed ends densities by those of active barbed ends, and the equations for the pointed ends do not change at all.

Further perturbations. Since there are about fifty different proteins known or suspected to be involved in actin dynamics one can consider many additional variations of the model. However, we are looking for a minimal model for the initiation of motion, and so we do not treat effects like filament branching, monomer sequestering, or filament severing at all, even if they may be important for the maintenance of movement.

4. Results and Conclusions

The perturbations described in the previous section show quite different effects which – as we will see in the following sections – strongly depend on the value of the diffusion coefficient D for the monomers.

4.1. **Monomer Perturbation.** The first observation is that it does not make a qualitative difference whether we release additional monomers or let the cell redistribute the existing ones. Also the choice of the type of steady state distribution for the pointed ends does not play an essential role for the results of these kind of perturbations, presumedly due to the slow reaction kinetics at the pointed ends.

Effect of different values for the diffusion coefficient. Under physiological conditions (i.e., default parameter values) or with an even higher diffusion coefficient the relaxation of the inhomogeneous monomer distribution to a flat distribution is so fast that the effect on the barbed ends is only small. The behavior of some important variables upon an asymmetric perturbation of the monomer concentration is shown in Table A1 in the appendix. Before the perturbation is applied at $t = 1.25\,s$ the system is in a steady state where none of the variables underlies temporal variations.

Chart *a)* shows the density of right oriented barbed ends, which is shifted toward the right boundary indicating a drift of barbed ends toward the cell membrane. In chart *b)* one can see that the density of left oriented barbed ends is hardly affected by the stimulus applied to the opposite side of the cell. So the asymmetric perturbation indeed induces an asymmetric response. The charts *c)* and *d)* show increasing densities of both, right and left oriented filaments due to filament elongation by the additional monomers supplied as perturbation. Again the effect on the right oriented species is bigger. The behavior of the monomer concentration can be seen in chart *e)*. Obviously the default diffusion coefficient $D = 30\,\mu m^2 s^{-1}$ causes a fast equilibration of the monomer density.

Noteworthy is the effect in case the diffusion coefficient is tenfold decreased compared to the default setting, i.e. $D = 3\,\mu m^2 s^{-1}$. As can be seen in chart *f)* of Table A1 the accumulated monomers then remain much longer close to their initial location and therefore allow for a faster growth of the barbed ends near the peak of the monomer distribution. We observe a significant agglomeration of filament ends growing towards the cell membrane shown in chart *g)*. The left oriented barbed ends are now even less affected as in the previous setting. Now the question emerges how this can be explained biologically. In fact there are current experimental results indicating a very slow diffusion of actin monomers in actin gels in vitro (see [17]). Possible explanations are the slowdown of diffusive motion due to temporary attachments of the monomers to the filament network or the presence of active transport of G-actin against the concentration gradient counteracting the diffusive effects.

4.2. **Variable Reaction rates and Critical Concentrations.** Possible variations of the critical concentrations are naturally constrained by the postulation $a_{crit.} > 0$. Since $a_B = 0.2a^{ss}$ the term $a - a_B$ cannot be increased significantly by decreasing a_B, and the growth of the barbed ends to the right will not be sufficient to enable the cell to start moving within a few seconds. The simulation

shows precisely that, i.e., we do not observe a notable effect on the end distribution upon a perturbation of the critical concentrations, independently of the choice of the diffusion coefficient or the choice of steady state distributions – at least within the range we have considered here.

The situation for variable reaction rates is quite different. We can observe a drift of barbed ends toward the right cell boundary caused by a locally increased barbed end velocity. Here the value of the diffusion coefficient plays an important role again. An increased reaction rate for the barbed ends leads to an enhancement of polymerization and therefore to a local depletion of monomers. The supply with new monomers happens by diffusion and is much faster the larger the diffusion coefficient is. Under these conditions the drift of barbed ends toward the cell membrane is incrementally stronger. However we can observe the desired effect of barbed ends accumulating near the membrane even for small diffusion coefficients since the simulation time is not as long as to allow for a momentous depletion of monomers.

4.3. **Combination of Several Perturbations.** One may expect that the cell combines several mechanisms. This can be easily simulated and shows an impressive outcome. Though we have used each single perturbation in a much weaker manner than before the effect is enormous. We give some exemplary charts in TABLE A2 in the appendix. The perturbations on monomer concentration and reaction kinetics are now applied at $t = 0.625\,s$. In chart *a)* we observe that some right oriented barbed ends have overcome the initial distance of $1.5\,\mu m$ to the cell membrane within less than $2\,s$. This results in a breakdown of the numerical code where homogeneous boundary conditions are imposed which produce artificial oscillations in the solution at that stage. The left oriented barbed ends in chart *b)* show nearly no effect at all. Chart *c)* shows an even more pronounced accumulation of barbed ends near the cell membrane if the diffusion coefficient is decreased to $D = 3\,\mu m^2 s^{-1}$.

Charts *d)* to *g)* show some results for symmetrically applied perturbations. We see from *d)* and *e)* that the response is indeed symmetric in this case but somewhat weaker than in the asymmetric setting which is in accordance to the expectations for a cell preparing to spread on a uniformly coated surface compared to one preparing to crawl rapidly.

The effect of a decreased diffusion coefficient is again a more distinct accumulation of barbed ends near the membrane as seen in chart *f)*. Chart *g)* shows the decreasing density of right oriented filaments which is also observed in the other settings with combined perturbations. The reason is the enhanced depolymerization at the pointed ends. Nonetheless the filaments do again follow the barbed ends toward the respective membrane.

As in the previous cases we do not find a notable difference between the effects on different kinds of steady states.

4.4. **Capping.** The expected effect of local barbed end capping is a local increase of the monomer density due to the existence of fewer free barbed ends which use up monomers by polymerization. This does not seem to play a crucial role in our given model. Even a very high capping rate does not influence the monomer concentration significantly.

It may be possible that the depletion of monomers caused by polymerization at too many barbed ends plays an important role only in lamellipodia where the diffusion driven supply with new monomers is reduced because of the small cross section of the lamellipod and the expected tight packing of filaments where migrating monomers are temporarily attached once in a while which slows down the diffusion flow. We have seen in 4.2 that even for high reaction rates and resulting filament growth in the right half of the cell the decay in monomer density is not strong enough to approach the critical concentration a_B, that is, we do not observe a critical depletion of monomers which would have to be balanced by capping. However, our model cell is not yet in motion but

still in preparation and we cannot deduce any assertions about the further development of the computed densities. Besides the effects discussed here, capping proteins are suspected to play a role in the regulation of de novo nucleation of actin filaments by capping and thus inactivating actin trimers. In our model we do not consider nucleation so far, and thus cannot investigate this mechanism here. Instead we assume that the cell can control nucleation by some machinery not included in our model without considering the concrete mechanisms involved in this regulation process. It may be a future goal to incorporate several of these regulation mechanisms into the mathematical model.

5. Discussion and Outlook

We have discussed several mechanisms involved in the process enabling a polarized cell to prepare to move in a given direction. The strongest effects in our model were observed upon release or redistribution of monomers and variations of the reaction rates, and especially for very small diffusion of monomers. These lead to a significant accumulation of right oriented barbed ends near the right cell boundary which should be able to push the membrane forward in, thus generating a protrusion. We thus may conjecture that a minimal model for cell motility will have to include some mechanism of regulating the reaction kinetics at least at the barbed ends which may be accomplished by sequestering agents. Also the release of additional monomers from a "hidden" pool could result from the inactivation of sequestering proteins inhibiting the polymerization of single actin monomers to filaments. However these additional monomers could also be newly expressed by local ribosomes or released from vesicles they have been stored in.

Whether and how the diffusion coefficient for monomers may be decreased in vivo remains to be determined. Possibly there are also other kinematic behaviors - such as active monomer transport - to be considered.

Under the basic assumptions of our model we found that no further ingredients than those mentioned above are needed to initiate the *preparation* for movement. In particular, barbed end capping, branching, and severing of filaments are apparently not essential for this impulse in the given context. However we cannot judge their relevance for the formation of protrusions and the maintenance of motion at later stages of the process. Another question we have not addressed so far is the interplay between all these mechanisms such as the regulatory effects of barbed end capping and branching on nucleation.

The processes involved in building a lamellipod may be investigated by reformulating our model into a free boundary problem where the barbed ends are allowed to hit the membrane whose movement would then be determined by the density and growth velocity of barbed ends there. In this setting the geometry of the cell will play an essential role and has to be considered more carefully.

Another extension of the model could be the introduction of additional dynamic variables representing sequestering protein or capper concentrations, leading to further equations and extensions of the given ones.

Furthermore, it would be nice to obtain (in vitro) experiments, supporting the results of the simulation.

Appendix

Tables. The following tables show the temporal behavior of the model variables upon a combination of the perturbations stated above. We have used the following parameters for the respective settings.

Steady state distributions:

$$B_{r,i} = 12000 \, \exp\left[\frac{0.75 \cdot 0.3^2}{(\frac{i}{N} - 0.8)^2 - 0.3^2}\right] \qquad for \; i = 0.325N, \ldots, \, 0.925N,$$

$$B_{r,i} = 0 \qquad otherwise.$$

$$B_{l,i} = B_{r,N-i}$$

and

$$P_{r,i} = P_{l,i} = \frac{1}{2}(B_{r,i} + B_{l,i})$$

Perturbations

monomer release:

always:

$$a_i = C \, a^{ss} \, \exp\left[\frac{3 \cdot 0.2^2}{(\frac{i}{N} - 0.8)^2 - 0.2^2}\right] \qquad for \; i = 0.6N, \ldots, \, N,$$

in symmetric case additionally:

$$a_i = C \, a^{ss} \, \exp\left[\frac{3 \cdot 0.2^2}{(\frac{i}{N} - 0.2)^2 - 0.2^2}\right] \qquad for \; i = 0, \ldots, \, 0.4N,$$

always:

$$a_i = a^{ss} \qquad otherwise$$

reaction rates:

symmetric case:

$$\kappa_i^B = 1.5 \, \kappa^{B,0} \left(\pi + \arctan\left[10\frac{i - 0.8N - 0.5}{N}\right] - \arctan\left[10\frac{i - 0.2N + 0.5}{N}\right]\right)$$

$$\kappa_i^P = \kappa^{P,0} \left(\pi - \arctan\left[10\frac{i - 0.7N - 0.5}{N}\right] + \arctan\left[10\frac{i - 0.3N + 0.5}{N}\right]\right)$$

asymmetric case:

$$\kappa_i^B = \kappa^{B,0} \left(\frac{\pi}{2} + \arctan\left[10\frac{i - 0.8N - 0.5}{N}\right]\right)$$

$$\kappa_i^P = \kappa^{P,0} \left(\frac{\pi}{2} - \arctan\left[10\frac{i - 0.7N - 0.5}{N}\right]\right)$$

critical concentrations:

symmetric case:

$$a_{B,i} = \frac{a_B^0}{\pi} \left(\pi - \arctan\left[5\frac{i - 0.8N - 0.5}{N}\right] + \arctan\left[5\frac{i - 0.2N + 0.5}{N}\right]\right)$$

$$a_{P,i} = \frac{a_P^0}{\pi} \left(\pi - \arctan\left[5\frac{i - 0.7N - 0.5}{N}\right] + \arctan\left[5\frac{i - 0.3N + 0.5}{N}\right]\right)$$

asymmetric case:

$$a_{B,i} = \frac{a_B^0}{\pi} \left(\frac{\pi}{2} - \arctan\left[5\frac{i - 0.8N - 0.5}{N}\right]\right)$$

$$a_{P,i} = \frac{a_P^0}{\pi} \left(\pi - \arctan\left[5\frac{i - 0.7N - 0.5}{N}\right]\right)$$

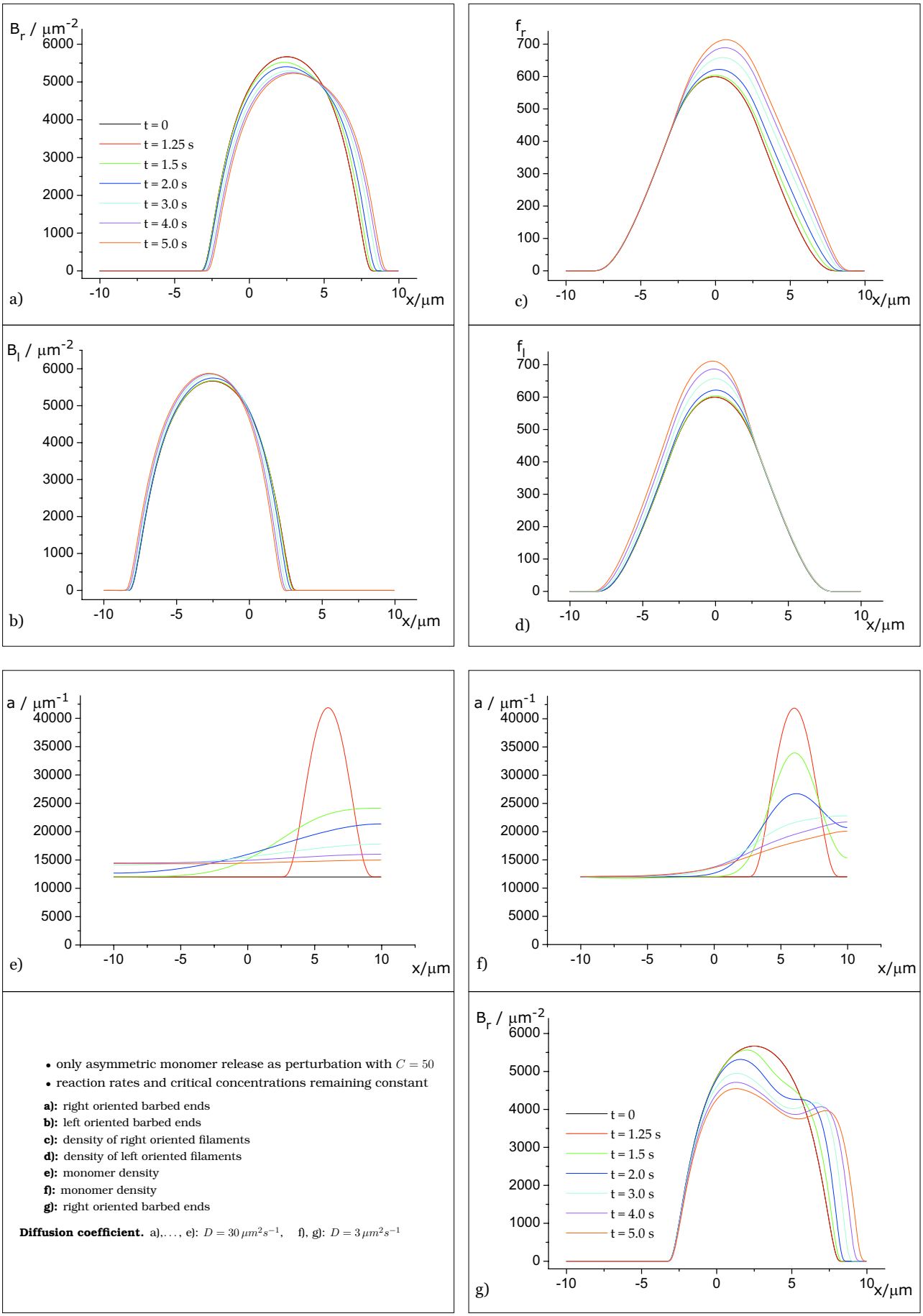

TABLE A1: Behavior of several densities upon monomer release. Note the significantly increased effect for the low diffusion coefficient (charts **f)** and **g)**)

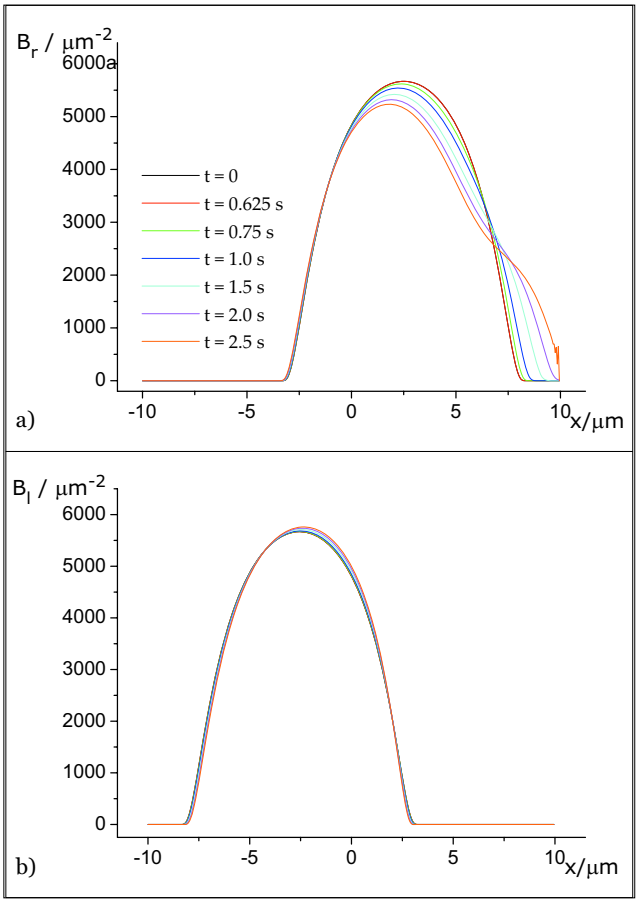

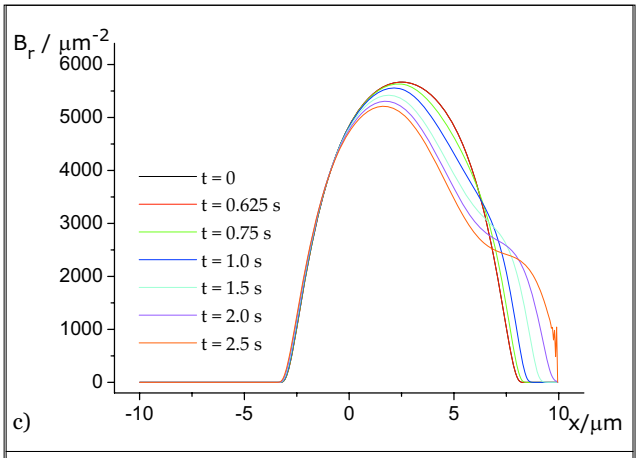

Combined perturbations

- monomer release as perturbation with $C = 20$
- reaction rates and critical perturbations also perturbed

a): right oriented barbed ends, $D = 30\ \mu m^2 s^{-1}$, asymmetric perturbations
b): left oriented barbed ends, $D = 30\ \mu m^2 s^{-1}$, asymmetric perturbations
c): right oriented barbed ends, $D = 3\ \mu m^2 s^{-1}$, asymmetric perturbations
d): right oriented barbed ends, $D = 30\ \mu m^2 s^{-1}$, symmetric perturbations
e): left oriented barbed ends, $D = 30\ \mu m^2 s^{-1}$, symmetric perturbations
f): right oriented barbed ends, $D = 3\ \mu m^2 s^{-1}$, symmetric perturbations
g): density of right oriented filaments, $D = 3\ \mu m^2 s^{-1}$, symmetric perturbations

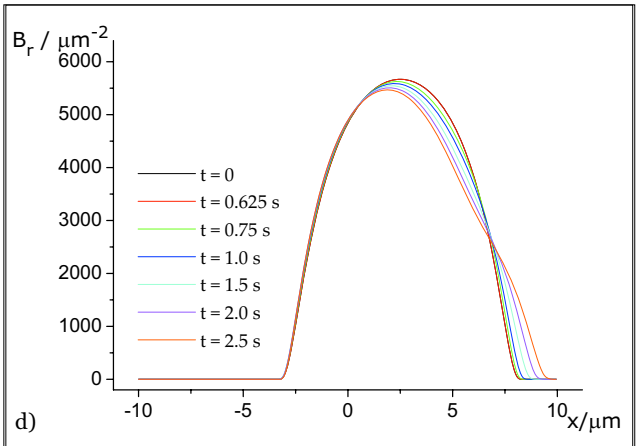

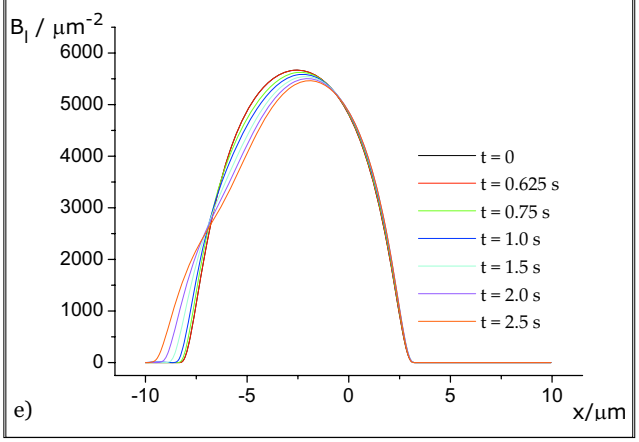

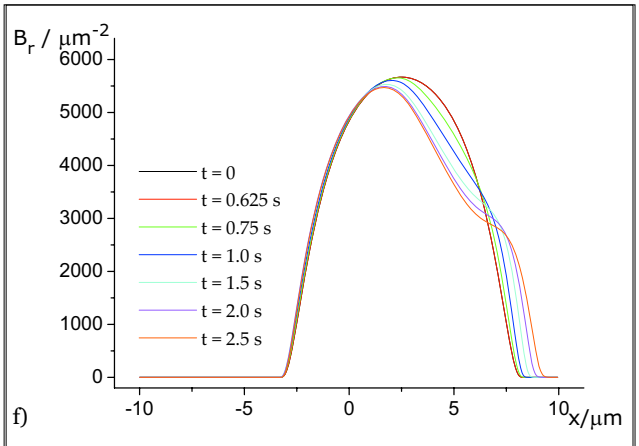

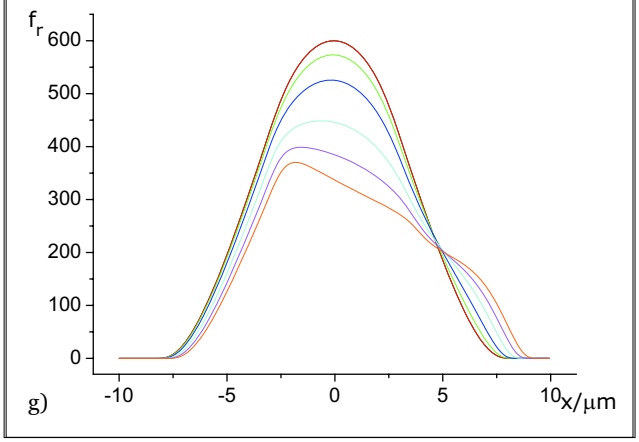

TABLE A2: Behavior of several densities upon a combination of different perturbations

Acknowledgement. Jan Fuhrmann is partially supported by the DFG (German Science Foundation) via the Graduate Research School InterNeuro.

References

[1] Alberts, B., et al., Molecular Biology of the Cell, 3^{rd} Ed. *Garland Publishing, Inc.* (1994)

[2] Allen, R. D. & Kamiya, N., Primitive Motile Systems in Cell Biology, *Academic Press* (1964)

[3] Alt, W. & Dembo, M., Cytoplasm Dynamics and Cell Motion: Two-Phase Flow Models, *Math. Biosciences* 156 (1999), 207-228

[4] Carlier, M. F., et al., Actin Based Motility: From Molecules to Movement, *BioEssays* 25 (2003, Wiley Periodicals, Inc.), 336-345

[5] Carlier, M. F. & Pantaloni, D., Control of Actin Dynamics in Cell Motility, *J. Mol. Biol.* 269 (1997), 459-467

[6] Chen, C. S., et al., Geometric Control of Cell Life and Death, *Science* 276 (30.05.1997), 1425 - 1428

[7] Cloney, R. A., Cytoplasmic Filaments and Cell Movements: Epidermal Cells During Ascidian Metamorphosis, *J. of Ultrastructure Research* 14 III+IV (1966), 300-328

[8] Döbereiner, H. G., et al., Dynamic Phase Transitions in Cell Spreading, *Phys. Rev. Lett.* 93, nr. 10 (2004) 108105

[9] Edelstein-Keshet, L. & Ermentrout, G. B., A Model for Actin-Filament Length Distribution in a Lamellipod. *J. Math. Biol.* 43 (2001), 325-355

[10] Gibbon, B. C., Actin Monomer-Binding Proteins and the Regulation of Actin Dynamics in Plants, *J. Plant Growth Regul.* 20 (2001), 103-112

[11] Goldman, R. D., Pollard, T., & Rosenbaum, J. (Eds.), Cell Motility. *Cold Spring Harbor* (1979)

[12] Jamney, P. A., The Cytoskeleton and Cell Signaling: Component Localization and Mechanical Coupling, *Physiological Reviews* 78 No. 3 (1998) 763-774

[13] Jurado, C., Haserick, J. R., & Lee, J., Slipping or Gripping? Fluorescent Speckle Microscopy in Fish Keratocytes Reveals Two Different Mechanisms for Generating a Retrograde Flow of Actin, *Molec. Biology of the Cell* 16 (2005), 507-518

[14] Mitchison, T. J. & Cramer, L. P., Actin Based Motility and Cell Locomotion, *Cell* 84 (1996)

[15] Mogilner, A. & Edelstein-Keshet, L., Control of Actin Dynamics in Rapidly Moving Cell: A Quantitative Analysis. *Biophys. J.* 83 (2002), 1237-1258

[16] Nabi, I. R., The Polarization of the Motile Cell, *J. of Cell Science* 112 (1999), 1803-1811

[17] Plastino, J., Lelidis, I., Prost, J., & Sykes, C., The Effect of Diffusion, Depolymerization and Nucleation Promoting Factors on Actin Gel Growth, *Eur. Biophys. J.* 33 (2004), 310-320

[18] Pollard, T. D. & Borisy, G. G., Cellular Motility Driven by Assembly and Disassembly of Actin Filaments, *Cell* 112 (2003), 453-465

[19] Rinaldi, R. A. & Baker, W. R., A Sliding Filament Model of Amoeboid Motion, *J. Theor. Biol.* 23 III (1969), 463-474